

Lawrence Berkeley National Laboratory

Recent Work

Title

Multilayer laminar-type diffraction gratings achieving high diffraction efficiencies in the 1-8 keV energy region

Permalink

<https://escholarship.org/uc/item/3hm8z3pg>

Journal

Applied Optics, 45(26)

Authors

Ishino, Masahiko
Heimann, Philip A.
Sasai, Hiroyuki
et al.

Publication Date

2006-04-12

Multilayer laminar-type diffraction gratings achieving high diffraction efficiencies in the 1-8 keV energy region

Masahiko Ishino, Philip A. Heimann*, Hiroyuki Sasai, Masatoshi Hatayama***, Hisataka Takenaka***, Kazuo Sano****, Eric M. Gullikson*, and Masato Koike**

Quantum Beam Science Directorate, Japan Atomic Energy Agency, 8-1, Umemidai, Kizu, Kyoto 619-0215, Japan,

** Lawrence Berkeley National Laboratory, 1 Cyclotron Road, Berkeley, CA 94720, USA*

*** Shimadzu Corp., 1-1, Nishinokyo-kuwabaramachi, Nakagyo, Kyoto 604-8511, Japan*

**** NTT Advanced Technology Co., 162 Shirakata-Shirane, Tokai, Naka, Ibaraki 319-1193, Japan*

***** Shimadzu Emit Co. Ltd., 2-5-23, Kitahama, Chuo, Osaka 541-0041, Japan*

Abstract

W/C and Co/SiO₂ multilayer gratings have been fabricated by depositing a multilayer coating on the surface of laminar-type holographic master gratings. The diffraction efficiency was measured by reflectometers in the energy region of 0.6-8.0 keV at synchrotron radiation facilities as well as at an x-ray diffractometer at 8.05 keV. The Co/SiO₂ and W/C multilayer gratings showed peak diffraction efficiencies of 0.47 and 0.38 at 4.0 and 8.0 keV, respectively. The peak efficiency of the Co/SiO₂ multilayer grating is the highest measured with hard x-rays, to our knowledge. The diffraction efficiency of the Co/SiO₂ multilayer gratings was higher than that of the W/C multilayer grating in the energy range of 2.5–6.0 keV. However, it decreased significantly in the energy above the K-absorption edge of Co (7.71 keV). For the Co/SiO₂ multilayer grating the measured

diffraction efficiencies agreed with the calculated curves assuming a rms roughness ~1 nm.

OCIS codes: 230.1950, 230.4170, 340.7480

1. Introduction

The *K*, *L* or *M* absorption edges of many elements including most of the transition metals are located in the energy region of 1–8 keV. Therefore spectroscopic research in this energy region is essential to investigate the atomic and electronic structure of these materials. Synchrotron radiation (SR) light sources having high brilliance and flux have been utilized for various experiments: for example, extended x-ray absorption fine structure (EXAFS)^{1,2} and x-ray absorption near edge fine structure (XANES).³

However, the throughput of the spectroscopic instruments employing diffraction gratings is usually not enough to perform these experiments satisfactory in this 2-8 keV energy region.⁴ Crystal spectrometers and monochromators usually based on Si crystals have been used in the energy region above 2 keV. These crystal spectrometers and monochromators provide good monochromaticity, but the integrated diffraction efficiency is limited by the narrow rocking curves of perfect crystals.

Multilayer coatings provide a way to increase the diffraction efficiency at a chosen incident angle. It has been performed either by coating a multilayer on a substrate having grating grooves.⁵⁻⁸ or forming grooves on a multilayer mirror.^{9,10} By kinematical theory the maximum diffraction efficiency for a multilayer grating is attained by satisfying the grating equation and extended Bragg condition simultaneously.¹¹

Multilayer gratings have been investigated in the energy regions below 2 keV and above 8 keV and most of them are carbon based multilayers such as Rh/C⁵, W/C^{6,9,10}, Mo/C¹⁰ and Pt/C.^{7,8} However, little work has been done to develop multilayer gratings in the energy region of 1–8 keV.^{10,12,13} Therefore we have developed multilayer laminar-type holographic gratings achieving a high diffraction efficiency in this energy region.

In this article we describe the selection of material pair, the fabrication of the multilayer gratings, and the evaluation of the diffraction efficiency by reflectometers at SR facilities as well as by an x-ray diffractometer.

2. Selection of Materials for Multilayer Coating

A multilayer grating is an optical device combining grating and multilayer structures. The primary goal of obtaining a high diffraction efficiency depends on finding a multilayer material pair having a high reflectivity.

We calculated the reflectivity of the 1st order Bragg peaks for multilayer mirrors composed of traditional material pairs, W/C,^{6,9,10} and Pt/C,^{7,8} as well as of new material pairs, Co/Si and Co/SiO₂, proposed from a systematic materials survey. Figure 1 shows the reflectivities of the multilayer mirrors vs. photon energy. The W/B₄C multilayer is also shown in Fig. 1 for comparison. Because it is reported that the W/B₄C multilayer has more stable structure and smoother interfaces than the W/C multilayer.^{14,15} The W/B₄C multilayer will be an alternative material pair for multilayer grating to the W/C multilayer. The calculated reflectivities of W/B₄C multilayer have almost the same values with those of W/C multilayer. To achieve the sufficient reflectivity for multilayer mirrors over the wide energy region, a multilayer period of 6.64 nm and 30 periods (60 layers) were chosen. The multilayer of 30 periods is enough to obtain a saturated reflectivity in the grazing incidence angles. The optical constants published by Henke *et al.* were used.¹⁶ Also the calculations assumed s-polarized x-rays incident on an ideal multilayer structure, i.e., uniform layer thickness and abrupt interfaces without roughness and inter-diffusion. The incidence angles (Bragg angles) were varied with the photon energy to satisfy the Bragg condition.

The W/C multilayer mirror shows the highest reflectivity at 8.0 keV, but the reflectivity drops around 2.0 keV because of the $M_{4,5}$ -absorption edges of tungsten at 1.81 keV. Similarly, the Pt/C multilayer exhibits a decrease in reflectivity near 2.5 keV resulting from the Pt $M_{4,5}$ -absorption edges at 2.1 to 2.2 keV. Furthermore the Co/SiO₂ multilayer achieves the highest reflectivity in the 3-7 keV energy region as shown in Fig. 1. The performance of Co/Si multilayer mirror is inferior to that of Co/SiO₂ in almost the entire energy region. The

reflectivity of both Co/SiO₂ and Co/Si multilayer mirrors decreases at 8.0 keV because of the *K*-absorption edge of Co at 7.71 keV.

For the Co/Si multilayer, the inter-diffusion between the Co and Si layers during deposition has been reported.¹⁷⁻²⁰ The inter-diffusion layers decrease the optical contrast of layer boundaries and may cause a deterioration in the reflectivity. To evaluate this effect we fabricated and measured the reflectivity of a Co/Si multilayer mirror at 8.05 keV, and obtained a considerably smaller reflectivity than the calculated one.

When used as a soft x-ray multilayer material SiO₂ is physically stable. For example it has been used successfully to improve the heat stability of Mo/Si multilayer mirrors.^{21,22} Therefore, the Co/SiO₂ and W/C multilayers are considered to be the most promising material pairs for our purpose.

3. Fabrication of multilayer gratings

Multilayer gratings were fabricated by depositing multilayers onto the surface of laminar-type holographic gratings. Figure 2 shows the schematic diagram of multilayer grating. For laminar-type grating, the planes of land and valley are parallel to the average grating surface. The widths of land and valley are *a* and *b*, respectively. The groove density of grating is given by $1/D$ and the groove depth is shown by *h* in Fig. 2. The multilayer having the periodic length *d* is deposited onto the grating surface. The fabrication process of the laminar-type holographic gratings was performed at Shimadzu Corp., Kyoto, Japan. The grating substrates were made of synthetic fused quartz. The size and surface roughness of the substrates were 40x40 mm² and 0.35 nm rms, respectively. A He/Cd laser ($\lambda = 441.6$ nm) and photoresist, OFPR5000, were used to make the photo resist pattern of 1200 lines/mm grooves on the surface of the grating substrate. The pattern was used as a mask to rule the laminar-type grooves on the substrate by reactive ion beam etching using CHF₃. For the W/C multilayer grating the groove depth (*h*) was 3 nm with a land to period ratio

(a/D) of 0.45. Similarly for the Co/SiO₂ multilayer grating the groove depth was 4 nm while the land to period ratio was 0.50.

The W/C multilayer was deposited at NTT Advanced Technologies Co. Ibaraki, Japan by the magnetron sputtering method. The Co/SiO₂ multilayer was coated at the Japan Atomic Energy Agency, Kyoto, Japan by the ion beam sputtering method. It is advantageous to use the magnetron sputtering method to fabricate the multilayer consisting of carbon layer, because the deposition rate for carbon is higher than that of the ion beam sputtering method. The nominal multilayer period length was 6.64 nm and the ratio of (W or Co thickness)/(periodic length) was 0.4. For the W/C multilayer, 50 periods were deposited while 30 periods were deposited for the Co/SiO₂ multilayer.

To examine the resultant period length of the multilayers, x-ray reflectivity measurements were carried out in the standard θ - 2θ scan mode by use of an x-ray diffractometer with a Cu- $K\alpha$ (8.05keV) source. To avoid appear the diffraction peaks from grating grooves, the direction of grooves was set to be parallel to the direction of incidence x-rays. The period lengths of multilayers deposited on the gratings were estimated by the Bragg peak positions. The multilayer period lengths were found to be 6.66 nm for the W/C multilayer grating and 6.62 nm for the Co/SiO₂ multilayer grating.

4. Results and Discussion

The diffraction efficiencies of both multilayer gratings were measured by a diffractometer with a Cu- $K\alpha$ (8.05keV) source and by a reflectometer at the Advanced Light Source (ALS) beamline 5.3.1²³ in the energy range of 2.5–8.0 keV. Also the diffraction efficiency in the energy region of 0.6–1.5 keV was measured at the SR Center of Ritsumeikan University BL-11²⁴ as well as at ALS BL 6.3.2.²⁵ All the diffraction efficiency measurements were performed for the first diffraction order ($m = +1$).

Figure 3 shows a schematic diagram of the experimental setup. Monochromatic x-rays

illuminated the multilayer gratings with the incidence angle α , and then the x-rays were diffracted with the diffraction angle β . The intensity of diffracted x-rays was measured by the detector via detector angle scan (θ_D). To obtain the maximum efficiency of diffracted x-rays, the incidence angle α was adjusted around the predicted optimal angle by the calculation.

Figure 4 shows the measured diffraction efficiency of W/C and Co/SiO₂ multilayer gratings. The decrease in efficiency of the W/C multilayer grating around 2.5 keV is attributed to the $M_{4,5}$ -absorption edge of tungsten at 1.81 keV. In the higher energy region, it increases with photon energy and reaches 0.38 at 8.0 keV. This value measured at ALS BL5.3.1 is consistent with the efficiency of 0.37 obtained at 8.05 keV by the Cu- K_α diffractometer.

On the other hand, the Co/SiO₂ multilayer grating shows higher performance than the W/C multilayer grating in the 2.5-6.0 keV region. Diffraction efficiencies of 0.41 were observed at 4.0 keV and 0.47 at 6.0 keV. However, the efficiency at 8.0 keV decreases to 0.14. Also, the efficiency decreases steeply from 4.0 keV to 2.5 keV. This photon energy dependence is understood from the K -absorption edges of Co (7.71 keV) and Si (1.84 keV).

Figure 5 shows the measured and calculated efficiencies of the zero-th ($m = 0$) and first ($m = +1$) orders of the Co/SiO₂ multilayer grating between 2.5 and 8.0 keV. Similarly, figure 6 shows the measured and calculated efficiencies of the W/C multilayer grating. The black circles and squares show the measured diffraction efficiencies of the zero-th and +1st orders, respectively. The solid curves indicate the calculated ideal diffraction efficiencies for the zero-th and +1st orders ($m = 0, +1$).

The theoretical diffraction efficiencies were calculated by use of a simulation code²⁶ based on differential methods. We have confirmed the validity of this code by reproducing the results of the previous work based on the dynamical and electromagnetic theories.^{27,28} The index of refraction derived from the atomic scattering factors was used.¹⁶ In the

calculation, smooth surfaces and abrupt interfaces were assumed. The multilayer period length was chosen to be the value measured by x-ray diffraction, i.e., 6.62 nm for the Co/SiO₂ multilayer and 6.66 nm for the W/C multilayer.

The difference between the measured and theoretical efficiency could be attributed to the surface roughness at the top and at the boundaries inside the multilayer. In addition, exotic layers may be generated by inter-diffusion at the boundaries.¹⁷⁻²⁰ To estimate the magnitude of these effects we applied the Debye-Waller factor,²⁹

$$R = R_0 \exp[-(4\pi\sigma \cos \alpha / \lambda)^2], \quad (1)$$

to the ideal theoretical diffraction efficiencies. R_0 is reflectivity of multilayer assuming an ideal structure at the incidence angle α at wavelength λ , and σ is the rms roughness of the interfaces. The efficiencies calculated for a rms surface roughness (σ) of 0.7, 1.0, and 1.3 nm are shown by dot-dashed curves. The comparison of the measured and theoretical efficiencies of the +1 order suggests that both multilayer gratings have a rms roughness of ~1 nm.

For the laminar gratings, the zero-th order efficiencies can be suppressed by controlling the groove depth.³⁰ This groove depth condition to suppress the zero-th order efficiency by the destructive interference is described by

$$\lambda / 2 = 2h \cos \alpha. \quad (2)$$

The groove depth of Co/SiO₂ multilayer grating was 4 nm, and then the wavelength calculated from Eq. (2) is around 0.33 nm (about 3.8 keV). The measured efficiency of zero-th order for Co/SiO₂ multilayer grating has a minimum at 4.0 keV, which is consistent with the theoretical prediction. For the W/C multilayer grating, the groove depth was 3 nm, so that the measured efficiency of zero-th order will have a minimum at < 2 keV. These results support that the condition to suppress the zero-th order light is also valid for the laminar-type multilayer gratings.

The measured zero-th order efficiencies are systematically higher than the calculated

values. This discrepancy might imply a different roughness effect, which is not included in the Debye-Waller factor, but reduces the suppression of the zero-th order.

5. Conclusion

Multilayer gratings have been fabricated with Co/SiO₂ and W/C multilayers on the surface of laminar-type holographic gratings. The goal was to achieve high diffraction efficiencies in the energy region of 1–8 keV. The Co/SiO₂ multilayer grating showed a high diffraction efficiency of over 0.4 in the energy range of 4–6 keV. However, in both the lower and higher energy regions the diffraction efficiency decreased below 0.2 because of *K*-absorption edges of silicon and cobalt. By contrast, the W/C multilayer grating showed a high efficiency of nearly 0.4 at 8 keV. The peak efficiencies measured here are the highest grating efficiencies observed at hard x-ray photon energies, to our knowledge. In conclusion, the use of a combination of Co/SiO₂ and W/C multilayer gratings is a promising approach to extend the capabilities of grating monochromators through the 1–8 keV energy region.

Acknowledgements

The authors are grateful to Dr. E. Glover and Mr. A. Aquila for their assistance in the measurements at ALS beamlines 5.3.1 and 6.3.2. The measurements carried out at the Advanced Light Source were supported by the Director, Office of Science, Office of Basic Energy Sciences, Materials Sciences Division, of the U.S. Department of Energy under Contract No. DE-AC03-76SF00098 at Lawrence Berkeley National Laboratory.

References

1. D. C. Koningsberger, X-Ray Absorption: Principles, Applications, Techniques of Exafs, Sexafs and Xanes (R. Prins ed., Wiley, New York, 1988).
2. F. Sette, S. J. Pearton, J. M. Poate, and J. E. Rowe, "Local structure of S impurities in GaAs," Phys. Rev. Lett. **56**, 2637-2640 (1986).
3. J. C. Fuggle, J. E. Inglesfield, Unoccupied Electronic States: Fundamentals for Xanes, Eels, Ips and Bis (Springer, Berlin, 1992).
4. P. A. Heimann, M. Koike, and H. A. Padmore, "Dispersive x-ray absorption spectroscopy with gratings above 2 keV," Rev. Sci. Instrum. **76**, 063102 (2005).
5. T. W. Barbee, Jr., "Combined microstructure x-ray optics (invited)," Rev. Sci. Instrum. **60**, 1588-1595 (1989).
6. J. C. Rife, T. W. Barbee, Jr., W. R. Hunter, and Cruddace, "Performance pf a tungsten/carbon multilayer-coated, blazed grating from 150 to 1700 eV," Physica Scripta **41**, 418-521 (1990).
7. E. Ishigro, T. Kawashima, K. Yamashita, H. Kunieda, T. Yamazaki, K. Sato, M. Koeda, T. Nagano, and K. Sano, "Multilayer coated laminar grating in the soft x-ray region," Rev. Sci. Instrum. **66**, 2112-2115 (1995).
8. T. Yoshioka, K. Yamashita, H. Kunieda, K. Tamura, A. Furuzawa, M. Watanabe, and K. Haga, "Development of multilayer coated gratings for high energy x-ray spectroscopy," Astron. Nachr. **320**, 384 (1999).
9. V. V. Martynov, H. A. Padmore, A. Yakshin, and Yu. A. Agafonov, "Lamellar multilayer gratings with very high diffraction efficiency," Proc. SPIE **3150**, 2-8 (1997).
10. V. V. Martynov, and Yu. Platonov, "Deep multilayer gratings with adjustable bandpass for spectroscopy and monochromatization," Rev. Sci. Instrum. **73**, 1551-1553 (2002).
11. W. K. Warburton, "On the diffraction properties of multilayer coated plane gratings," Nucl. Instrum. Methods Phys. Res. A **291**, 278-285 (1990).

12. I. McNulty, Y. P. Feng, S. P. Frigo, T. M. Mooney, "Multilayer spherical grating monochromator for 1-4 keV x-rays," Proc. SPIE **3150**, 195 – 204 (1997).
13. M. Koike, M. Ishino, and H. Sasai, "Design of a high efficiency grazing incidence monochromator with multilayer coated laminar gratings for the 1-6 keV region," Rev. Sci. Instrum. **77**, 023101 (2006).
14. A. F. Jankowski, L. R. Schrawyer, M. A. Wall, W. W. Craig, R. I. Morales, and D. M. Makowiecki, "Interfacial bonding in W/C and W/B₄C multilayers," J. Vac. Sci. Technol. A **7**, 2914-2918 (1989).
15. A. F. Jankowski, L. R. Schrawyer, and M. A. Wall, "Structural stability of heat-treated W/C and W/B₄C multilayers," J. Appl. Phys. **68**, 5162-5168 (1990).
16. B. L. Henke, E. M. Gullikson, and J. C. Davis, "X-ray interactions: photoabsorption, scattering, transmission, and reflection at E = 50 – 30,000 eV, Z = 1 – 92," At. Data Nucl. Data Tables **54**, 181-342 (1993).
17. P. Ruterana, P. Houdy, and P. Boher, "A transmission electron microscopy study of low-temperature reaction at the Co-Si interface," J. Appl. Phys. **68**, 1033-1037 (1990).
18. H. Miura, E. Ma, and V. Thompson, "Initial sequence and kinetics of silicide formation in cobalt/amorphous-silicon multilayer films," J. Appl. Phys. **70**, 4287-4294 (1990).
19. J. Y. Shim, S. W. Park, and H. K. Baik, "Silicide formation in cobalt/amorphous silicon, amorphous Co-Si and bias-induced Co-Si films," Thin Solid Films **292**, 31-39 (1997).
20. J. M. Fallon, C. A. Faunce, and P. J. Grundy, "Microstructure of sputter-deposited Co/Si multilayer thin films," J. Appl. Phys. **88**, 2400-2407 (2000).
21. M. Ishino, O. Yoda, H. Takenaka, K. Sano, and M. Koike, "Heat stability of Mo/Si multilayers inserted with compound layers," Surf. Coat. Technol. **169-170**, 628-631 (2003).
22. M. Ishino and O. Yoda, "Optimization of the silicon oxide layer thicknesses inserted in the Mo/Si multilayer interfaces for high heat stability and high reflectivity," J. Appl.

- Phys. **92**, 4952-4958 (2002).
23. P. A. Heimann, A. M. Lindenberg, I. Kang, S. Johnson, T. Missalla, Z. Chang, R. W. Falcone, R. W. Schoenlein, T. E. Glover, and H. A. Padmore, "Ultrafast x-ray diffraction of laser-irradiated crystals," Nucl. Instrum. Methods. Phys. Res. A **467-468**, 986-989 (2001).
24. M. Koike, K. Sano, O. Yoda, Y. Harada, M. Ishino, N. Moriya, H. Sasai, H. Takenaka, E. Gullikson, S. Mrowka, M. Jinno, Y. Ueno, J. H. Underwood, and T. Namioka, "New evaluation beamline for soft x-ray optical elements," Rev. Sci. Instrum. **73**, 1541-1544 (2002).
25. J. H. Underwood, E. M. Gullikson, M. Koike, and P. J. Batson, "Beamline for metrology of x-ray/EUV optics at the Advanced Light Source," Proc. SPIE **3113**, 214-221 (1997).
26. GSOLVER V4.2b, Grating Solver Development Co., Allen, Texas.
27. B. Pardo, J. -M. Andrè, and A. Summar, "Dynamical theory of diffraction at in-depth multilayered gratings," J. Optics **22**, 141-148 (1991).
28. M. Nevière, "Bragg-Fresnel multilayer gratings: electromagnetic theory," J. Opt. Soc. Am. A **11**, 1835-1845 (1994).
29. E. Spiller, Soft X-ray Optics (SPIE Press, Bellingham, WA, 1994).
30. K. -H. Hellwege, "Über rasterförmige Reflexionsgitter," Z. Phys, **106**, 558-596 (1937).

Figure Captions

FIG. 1. First order Bragg reflectivities calculated for various multilayer mirrors. A 6.64 nm period length and 30 periods were assumed for the multilayers. Calculations are made for s-polarized x-rays and ideal multilayer structures. The incidence angles were varied with the photon energy to satisfy the Bragg condition.

FIG. 2. Schematic diagram of multilayer grating.

FIG. 3. Geometry of experimental setup for efficiency measurements. α : incidence angle, β : diffraction angle, and θ_D : detector angle.

FIG. 4. The measured diffraction efficiencies of the W/C and Co/SiO₂ multilayer gratings.

FIG. 5. The measured and calculated efficiencies are compared for the Co/SiO₂ multilayer grating. Results for the zero-th and first diffraction orders ($m = 0, +1$) are shown. The symbols show the measured diffraction efficiencies and the lines indicate the calculated diffraction efficiencies with various Debye-Waller factors.

FIG. 6. The measured and calculated efficiencies are compared for the W/C multilayer grating. Results for the zero-th and first diffraction orders ($m = 0, +1$) are shown. The symbols show the measured diffraction efficiencies and the lines indicate the calculated diffraction efficiencies with various Debye-Waller factors.

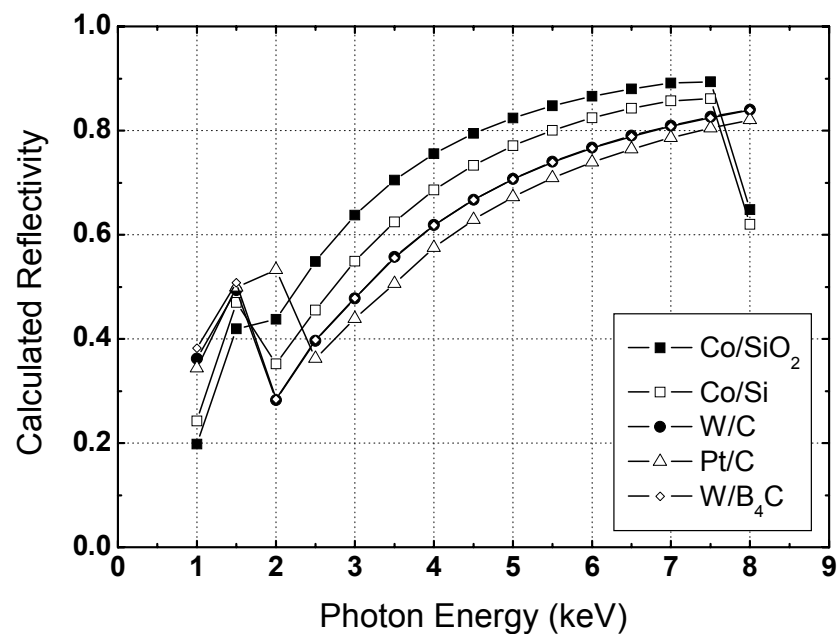


FIG. 1.

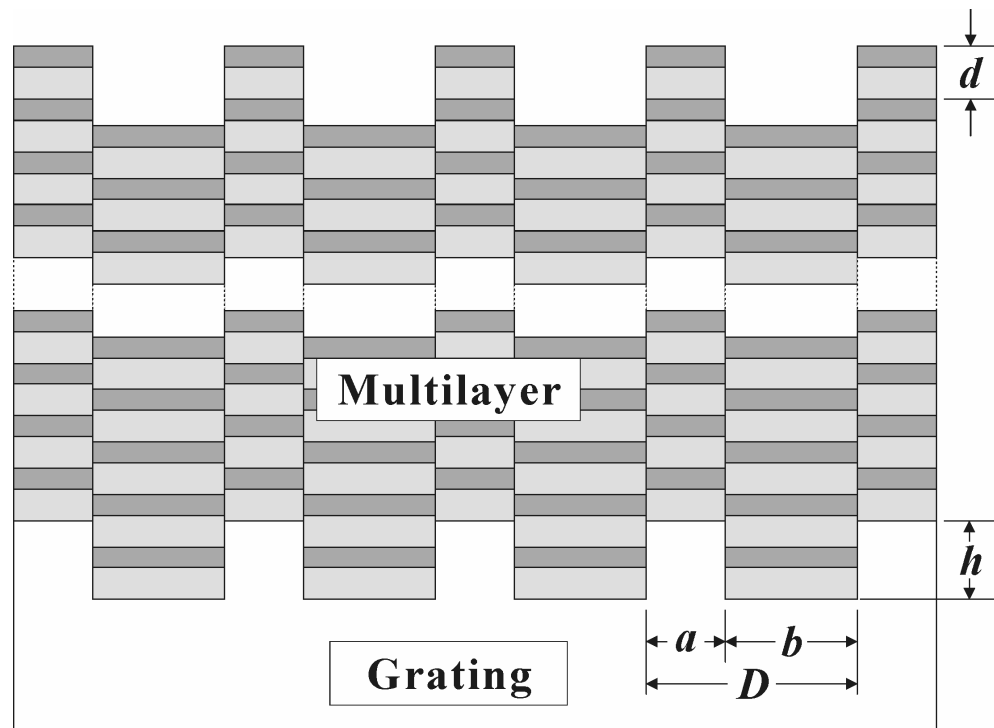


FIG. 2.

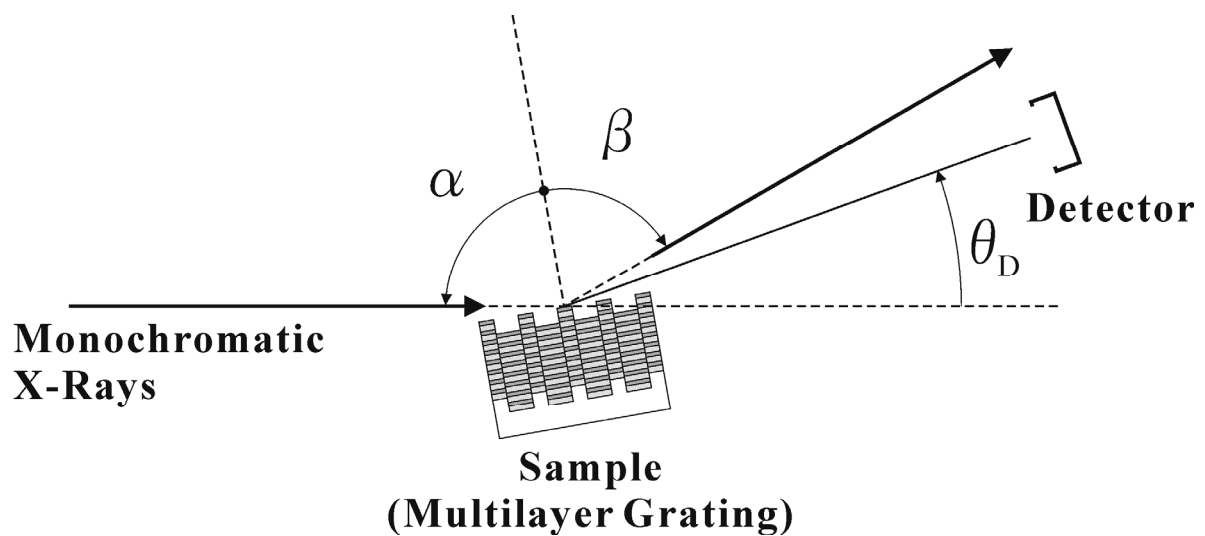


FIG. 3.

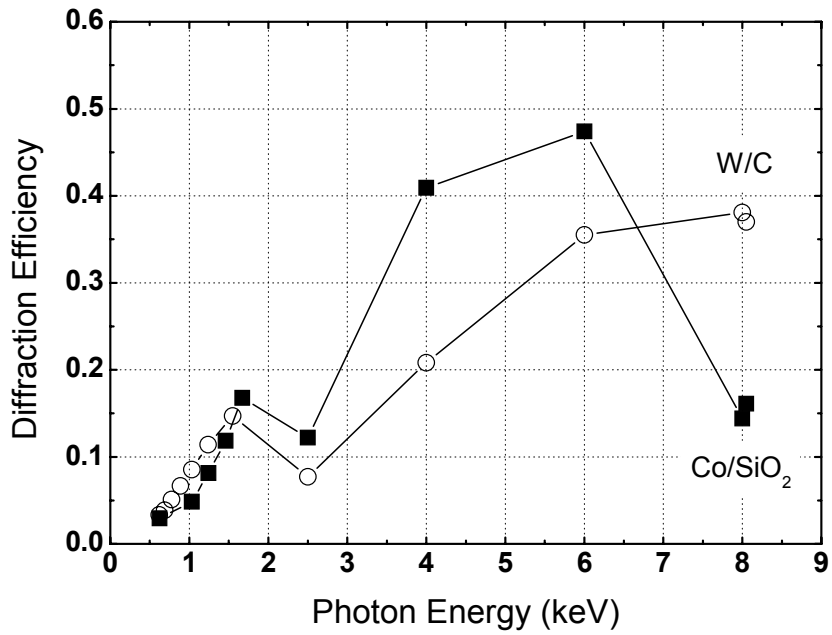


FIG. 4.

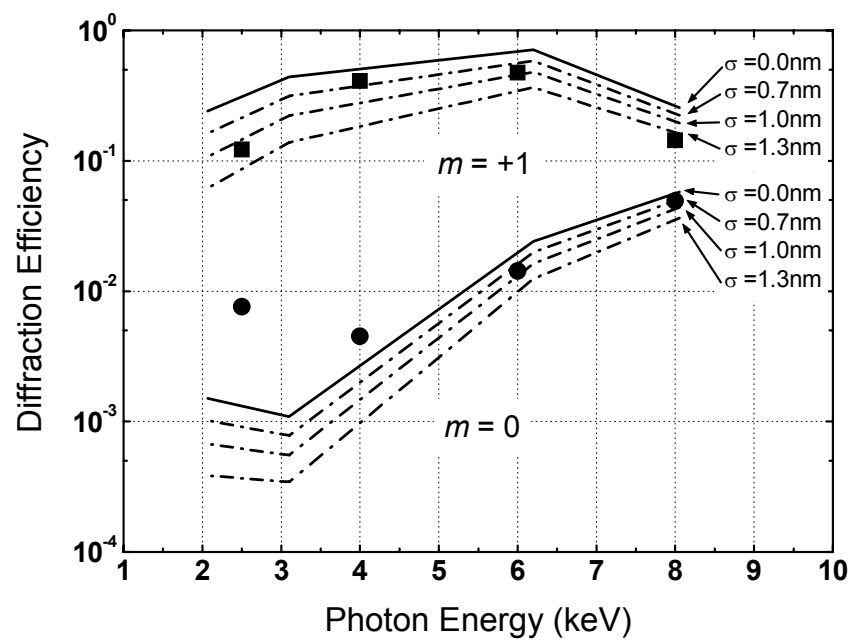


FIG. 5.

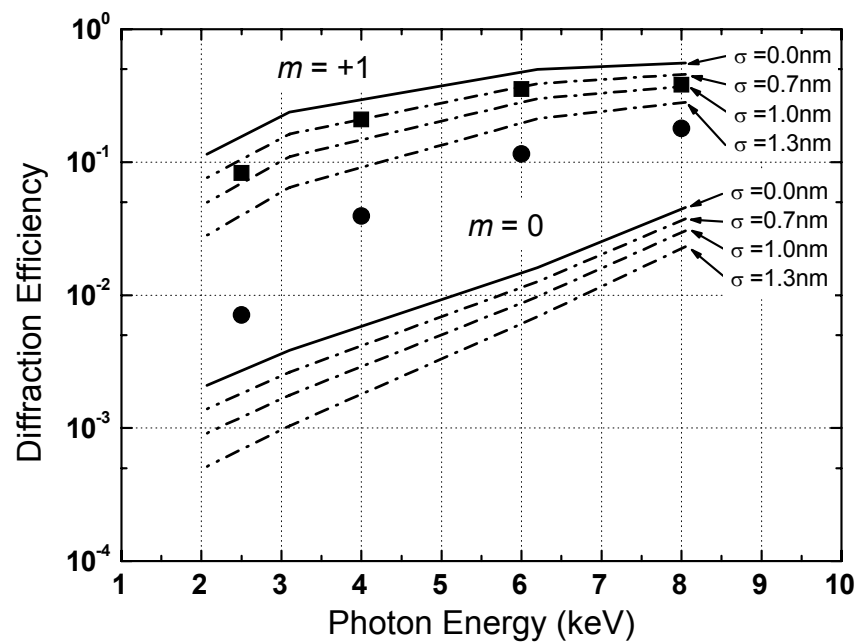


FIG. 6.